

COMBINATORIAL DESCRIPTION OF CLOSED 3-MANIFOLDS VIA ORDERED IDEAL TRIANGULATIONS

STAVROS GAROUFALIDIS, RINAT KASHAEV, AND SAKIE SUZUKI

ABSTRACT. It is well known that every compact oriented 3-manifold admits an ideal triangulation, and that any two such triangulations with at least two ideal tetrahedra are related by a sequence of Pachner 2–3 moves. Motivated by constructions in quantum topology, we give a combinatorial description of closed 3-manifolds in terms of ordered ideal triangulations and ordered Pachner 2–3 and 0–2 moves.

CONTENTS

1. Introduction	1
1.1. Ideal triangulations and ordered ideal triangulations	1
1.2. Ordered ideal triangulations for closed 3-manifolds	2
1.3. Moves for ordered ideal triangulations	3
1.4. Main results	4
1.5. Organization of the paper	5
Acknowledgments	5
2. Ordered ideal triangulations and normal o-graphs	5
3. Moves on normal o-graphs	6
3.1. MP moves and bumping MP moves	6
3.2. Pure sliding moves and bumping pure sliding moves	8
3.3. CP move	10
4. Main results and proofs in terms of normal o-graphs	10
4.1. Main results	10
4.2. Relations among moves	11
4.3. Proof of Proposition 4.4	14
References	16

1. INTRODUCTION

1.1. Ideal triangulations and ordered ideal triangulations. An ideal triangulation of a compact 3-manifold M with non-empty boundary is a decomposition of $\text{int}(M)$ into a collection of ideal tetrahedra with their faces glued in pairs, where an ideal tetrahedron is obtained by removing the four vertices of a tetrahedron. Ideal triangulations are combinatorial objects that were introduced and used by Thurston to describe the hyperbolic structure of knot complements [14], and have since become a fundamental tool in the study of the geometry, topology and quantum topology of 3-manifolds. Moreover, ideal triangulations have been implemented in software such as SnapPy [8] and Regina [6], providing effective tools for the classification of 3-manifolds and allowing for experimentation and visualization of phenomena in 3-dimensional topology.

A fundamental problem in this approach is to determine which local moves relate ideal triangulations representing the same 3-manifold. In particular, it is known that any two ideal triangulations of the same 3-manifold with at least two ideal tetrahedra are related by a sequence of Pachner 2–3 moves and their inverses [10]; see Figure 1.1.

Date: 28 May 2026.

Key words and phrases: 3-manifolds, triangulations, Pachner moves, ordered triangulations, normal o-graphs.

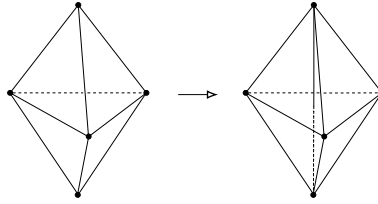


Figure 1.1. Pachner 2–3 move.

In this paper, we consider *ordered ideal triangulations* of compact, oriented 3-manifolds, that is, ideal triangulations in which each tetrahedron is equipped with a total ordering of its vertices and the face identifications preserve this ordering.

An ordered tetrahedron has two possible types, as shown in Figure 1.2, according to whether the vertex ordering is compatible with the orientation of the 3-manifold.

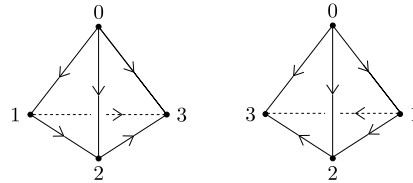


Figure 1.2. Two types of ordered ideal tetrahedra. The order is indicated by numbers on the vertices or by arrows (or both) pointing from smaller to larger vertices.

Ordered triangulations arise naturally in several contexts. In quantum topology, one assigns an operator to each tetrahedron using the ordering structure. For example, in the state-sum construction of the Turaev–Viro invariant [15], one assigns a $6j$ -symbol to each tetrahedron, where the $6j$ -symbol is obtained from an operator associated with an ordered tetrahedron via a symmetrization procedure (cf. [5]). In the construction of quantum invariants of framed 3-manifolds [11, 12], one assigns to each ideal tetrahedron an operator given by the canonical element of the Heisenberg double of a Hopf algebra. In particular, in quantum Teichmüller theory [1] and in the quantum hyperbolic invariant [3–5], one assigns to each ideal tetrahedron an operator derived from the Faddeev–Kashaev quantum dilogarithm, where the quantum dilogarithm arises from the canonical element of the Heisenberg double of the quantum Borel subalgebra $U_q(\mathfrak{sl}_2^+)$. All of these operators satisfy pentagon-type relations corresponding to the Pachner 2–3 move, just as the Yang–Baxter equation corresponds to the Reidemeister III move in quantum link invariants.

1.2. Ordered ideal triangulations for closed 3-manifolds. An ordered ideal triangulation determines not only a 3-manifold, but also a nowhere-vanishing vector field on it whose flow follows the ordering of the vertices of each tetrahedron, as shown in Figure 1.3.

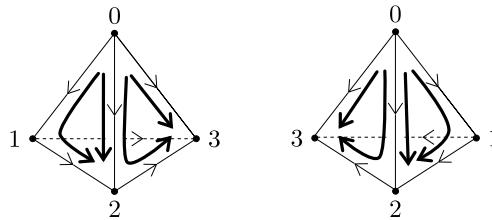


Figure 1.3. Ordered ideal tetrahedra with flows following the vertex ordering.

An ideal triangulation on M determines a triangulation of its boundary ∂M by truncating the tetrahedra at their vertices. An ordered triangulation determines a collection of arcs at these triangles, namely the

tangency locus of the above-mentioned vector field (shown in thick lines in Figure 1.4). The arcs join to a collection of multicurves on ∂M , which we call informally a *sutured structure* on ∂M .

In what follows, we assume that 3-manifolds are connected. To describe a closed 3-manifold M , we consider ideal triangulations of $M \setminus \text{int}(B^3)$.¹ In this setting, we restrict to ordered ideal triangulations with a standard sutured S^2 boundary as shown in Figure 1.4. Under this condition, the nowhere-vanishing vector field extends uniquely from $M \setminus \text{int}(B^3)$ to M .

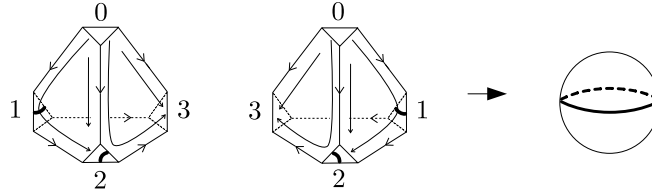


Figure 1.4. The standard sutured structure on S^2 : the multicurve is a single circle bounding two disks in S^2 .

Such vector fields on closed 3-manifolds have been studied from a combinatorial viewpoint via spines. In particular, Ishii [9] gave a combinatorial description of closed 3-manifolds using *flow spines*, which are spines arising from non-singular flows on closed 3-manifolds. There is a natural bijection between standard flow spines, where standard means special in the sense of [10], and ordered ideal triangulations with the standard sutured S^2 boundary. Benedetti and Petronio [2] also gave combinatorial descriptions of *combed* 3-manifolds and closed 3-manifolds using *closed normal o-graphs*, which provide graphical presentations of ordered ideal triangulations with the standard sutured S^2 boundary.

Muramatsu, Taguchi, and the third author [13] simplified the combinatorial descriptions of closed 3-manifolds by Benedetti–Petronio [2]. However, the description still involves the *combinatorial Pontryagin move* (in short, *CP move*), whose combinatorial structure is rather complicated.

In the present paper we replace the CP move with simpler local moves and obtain a local combinatorial description of closed 3-manifolds. In this introduction we formulate our main result in the language of ordered ideal triangulations, while further results and proofs will be carried out using the language of normal o-graphs.

1.3. Moves for ordered ideal triangulations. To give a combinatorial description of 3-manifolds, we consider two types of local moves on ordered ideal triangulations.

An *ordered 2–3 move* is the Pachner 2–3 move on the underlying triangulations such that the ordering of the vertices on each of the six boundary faces is preserved. See Figure 1.5 for the standard ordered 2–3 move.

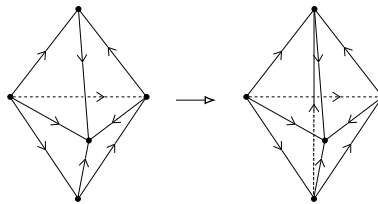


Figure 1.5. The standard ordered 2–3 move.

There are 20 types of ordered 2–3 moves. There are 16 combinatorial patterns before the move, and for 4 of them there are exactly two possible orientations of the common edge of the 3 tetrahedra.

An *ordered 0–2 move* inserts, along a pair of faces that share an edge, a ball triangulated by two ordered tetrahedra sharing two faces; see Figure 1.6. The ordering structure on the four triangles at the boundary of the inserted ball must agree with that of the corresponding faces.

¹Such ideal triangulations are also known as 1-vertex triangulations of M .

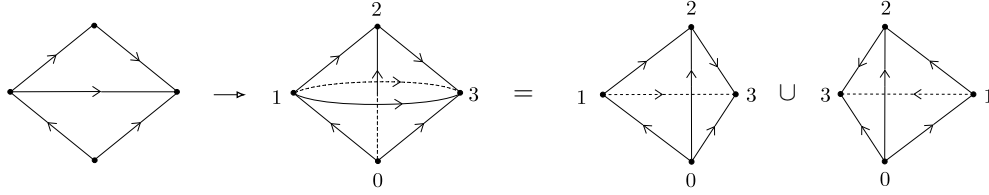


Figure 1.6. An ordered 0–2 move. The right-hand side consists of two ordered tetrahedra glued along two faces 012 and 023.

For a given pair of faces, the result of the ordered 0–2 move is unique, and there are 6 combinatorial patterns, see Figure 1.7.

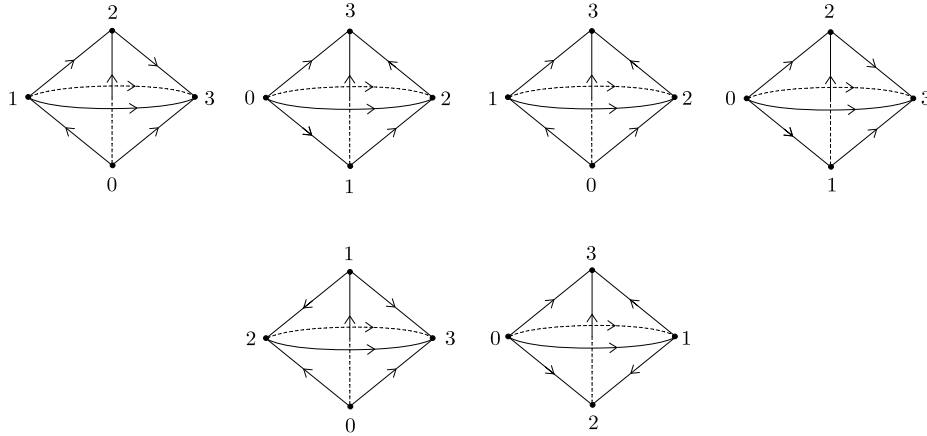


Figure 1.7. All 6 combinatorial types of ordered 0–2 moves.

1.4. Main results. We arbitrarily choose one ordered 2–3 move and call it the preferred move. The following theorem generalizes the result of [13].

Theorem 1 (Theorem 4.2 and Corollary 4.7). Each ordered 2–3 move can be realized as a sequence consisting of a single preferred ordered 2–3 move (or its inverse) together with ordered 0–2 moves and their inverses.

The main result of this paper is the following.

Theorem 2 (Theorem 4.5). The equivalence classes of ordered ideal triangulations with the standard sutured S^2 boundary, up to a single preferred ordered 2–3 move and ordered 0–2 moves, are in one-to-one correspondence with the orientation-preserving homeomorphism classes of closed 3-manifolds.

We remark that the two ordered 0–2 moves in the bottom row of Figure 1.7 change the sutured structure on the boundary (cf. [2, Figure 3.23]). The equivalence relation in Theorem 2 is the restriction of the equivalence relation on all ordered ideal triangulations to those with the standard sutured S^2 boundary.

Theorem 2 refines [7, Theorem 3.1], and gives an affirmative answer to a restricted version of [2, Question 9.1.4] for closed normal o-graphs, see Section 4.1 for details.

A natural generalization of Theorem 2 to compact 3-manifolds with torus boundary is an important problem.

Question 1. Consider ordered ideal triangulations with torus boundary, up to ordered 2–3 moves and ordered 0–2 moves. Do their equivalence classes correspond bijectively to the orientation-preserving homeomorphism classes of compact 3-manifolds with torus boundary?

This question is a reformulation of [2, Question 9.1.3] in terms of ordered ideal triangulations, in the torus boundary case.

1.5. Organization of the paper. The paper is organized as follows. In Section 2, we explain a diagrammatic description of ordered ideal triangulations using normal o-graphs. In Section 3, we describe the moves on ordered ideal triangulations in terms of normal o-graphs. In Section 4.1, we state the main result (Theorem 4.5) in terms of normal o-graphs. Section 4.2 is devoted to a detailed study of the precise relations among moves of normal o-graphs. In Section 4.3, we prove Proposition 4.4, which completes the proof of Theorem 4.5 (equivalently, Theorem 2 in the introduction).

Acknowledgments. We would like to thank the organizers of the workshop on “Low-dimensional Topology and Number Theory”, held at Oberwolfach in April 2026 for providing a stimulating environment. The work of RK is partially supported by the SNSF research program NCCR The Mathematics of Physics (SwissMAP), the SNSF grants no. 200021-232258, no. 200020-200400, and no. 10009199. The work of SS was partially supported by JSPS KAKENHI Grant Number JP24K06736.

2. ORDERED IDEAL TRIANGULATIONS AND NORMAL O-GRAPHS

A normal o-graph encodes a branched spine, which is dual to an ordered ideal triangulation. In this section we describe ordered ideal triangulations directly in terms of normal o-graphs, without referring to branched spines. For the theory of branched spines, see [2].

A *normal o-graph* is a finite connected 4-valent graph Γ with at least one vertex, equipped with the following additional structures:

- (1) Each vertex of Γ is endowed with an embedding of a neighborhood of the vertex into \mathbb{R}^2 , viewed up to planar isotopy. In addition, one pair of opposite edge germs is marked as passing over the other pair, as in a link diagram.
- (2) Each edge is oriented, and the orientations of opposite edges agree at each vertex.

Such a graph admits a planar diagram in \mathbb{R}^2 that realizes the prescribed local planar structures at the vertices. In general, virtual crossings are introduced as artifacts of the planar representation. There are two types of classical crossings, positive and negative, as for link diagrams. Two such planar diagrams represent the same normal o-graph if they are related by planar isotopy and the Reidemeister-type moves shown in Figure 2.1.

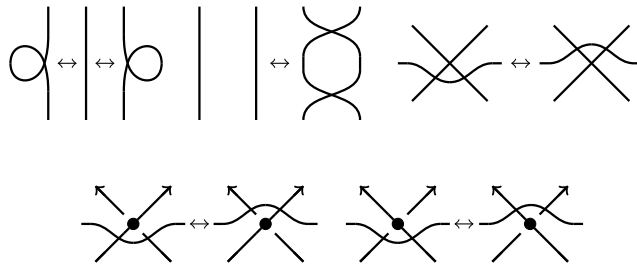


Figure 2.1. Reidemeister-type moves.

There is a one-to-one correspondence between normal o-graphs and ordered ideal triangulations, defined as follows.

Let Γ be a normal o-graph. For each positive (resp. negative) crossing of Γ , we associate an ordered tetrahedron of type $-$ (resp. type $+$) as shown in Figure 2.2, so that the four edges of the crossing correspond to the four faces of the ordered tetrahedron. We then obtain an ordered ideal triangulation by gluing the faces of these tetrahedra along the edges of Γ . This gluing is uniquely determined since it is required to preserve the ordering of vertices.

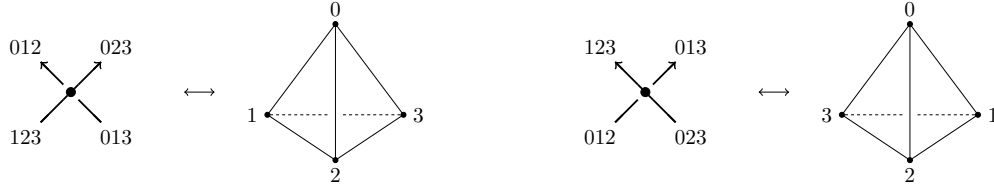


Figure 2.2. Correspondence between crossings of a normal o-graph and ordered tetrahedra. A positive crossing corresponds to an ordered tetrahedron of type $-$ (left), and a negative crossing corresponds to an ordered tetrahedron of type $+$ (right). The three numbers at each endpoint of the crossing indicate the face of the corresponding ordered tetrahedron. The tetrahedra are drawn in \mathbb{R}^3 .

The above construction is reversible; an ordered ideal triangulation uniquely determines a normal o-graph.

A *closed normal o-graph* is a normal o-graph representing an ordered ideal triangulation of a closed 3-manifold M with a ball removed, such that the associated vector field divides the spherical boundary into two hemispheres with ingoing and outgoing vectors. This closedness condition can also be described purely combinatorially in terms of normal o-graphs; see [2].

3. MOVES ON NORMAL O-GRAPHS

Recall that there are two types of moves on ordered ideal triangulations: the ordered 2–3 moves and the ordered 0–2 moves. We now recall the corresponding moves on normal o-graphs. If the induced move on ordered ideal triangulations preserves the sutured structure on the boundary, these moves are called *Matveev–Piergallini (MP) moves* and *pure sliding moves*. Otherwise, they are called *bumping MP moves* and *bumping pure sliding moves*.

3.1. MP moves and bumping MP moves. We translate the 20 types of ordered 2–3 moves on ideal triangulations in terms of normal o-graphs.

The *MP moves* on normal o-graphs are shown in Figures 3.1–3.4.

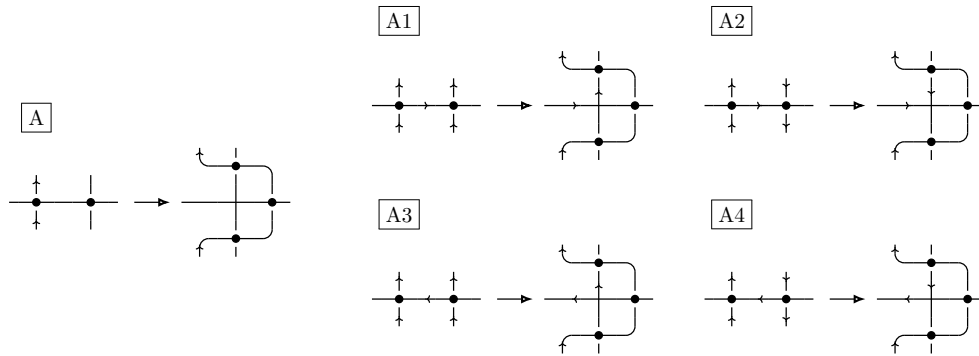


Figure 3.1. MP moves of type A.

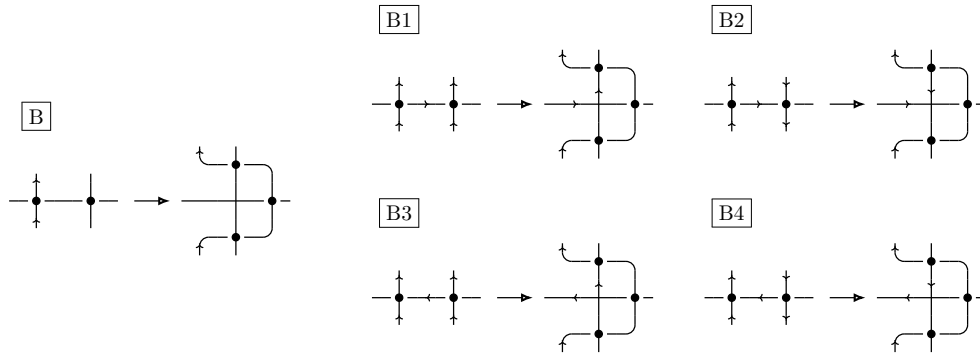


Figure 3.2. MP moves of type B.

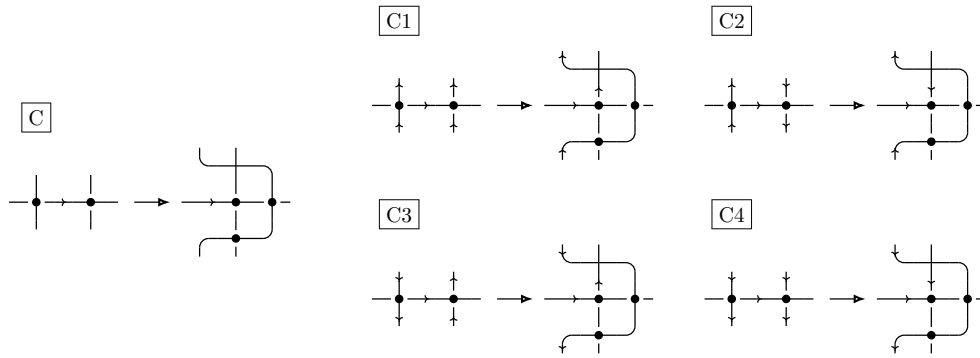


Figure 3.3. MP moves of type C.

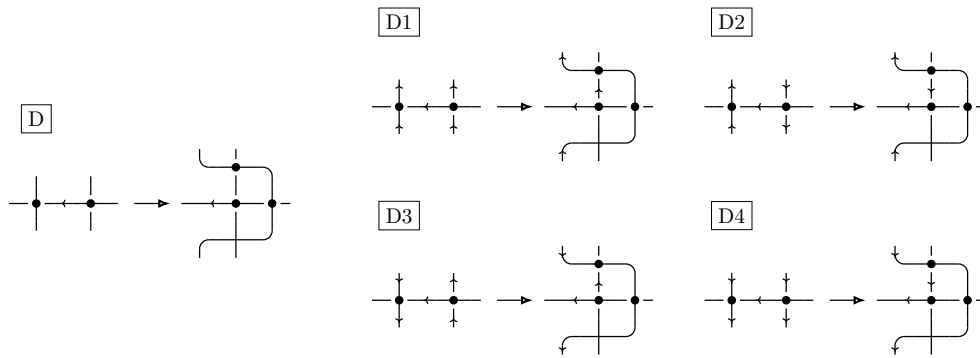


Figure 3.4. MP moves of type D.

The *bumping MP moves* on normal o-graphs are shown in Figure 3.5.

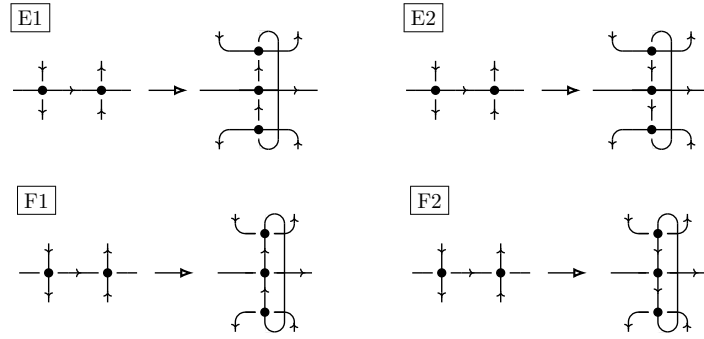


Figure 3.5. Bumping MP moves.

3.2. Pure sliding moves and bumping pure sliding moves. We translate the 6 types of ordered 0–2 moves on ideal triangulations in terms of normal o-graphs: the *pure sliding moves* and the *bumping pure sliding moves* on normal o-graphs, shown in Figure 3.6 and Figure 3.7, respectively.

The local graph on the left-hand side of each move does not contain enough combinatorial information to determine whether the corresponding two faces in the ideal triangulation share an edge or how they are attached. Therefore, we require certain global conditions on normal o-graphs in order to perform these moves.²

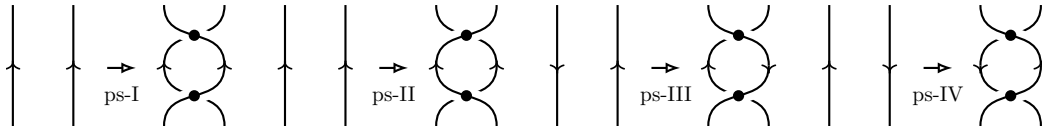


Figure 3.6. Pure sliding moves ps-I – ps-IV.



Figure 3.7. Bumping pure sliding moves.

We recall from [13] the conditions (PS-I)–(PS-IV) under which ps-I–ps-IV can be performed on normal o-graphs.

Given a diagram of a normal o-graph Γ , we construct immersed oriented closed curves in \mathbb{R}^2 as follows. First, we replace each true vertex of Γ with six immersed arcs, as illustrated on the left-hand side of Figure 3.8. Then we connect the endpoints of these arcs by arcs running parallel to the edges, as shown on the right-hand side of Figure 3.8. We call the resulting diagram the *circuit diagram* of Γ , following the construction in [2], as used also in [13]. For each edge, the three corresponding arcs in the circuit diagram are ordered from left to right when the edge is directed upwards.

²The pure sliding moves were introduced in [2] for branched spines and later formulated combinatorially on normal o-graphs in [13]. Bumping pure sliding moves for branched spines also appear in [2] and are formulated combinatorially on normal o-graphs in the present paper.

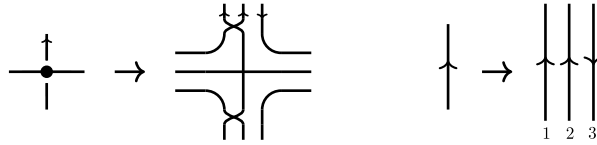


Figure 3.8. Circuit diagrams around a vertex (left) and an edge (right).

For each move ps-I–ps-IV, the two edges on which we perform the move must satisfy the corresponding condition on the circuit diagram, as follows:

- (PS-I) the third arc on the left is connected to the second arc on the right;
- (PS-II) the third arc on the left is connected to the first arc on the right;
- (PS-III) the first arc on the left is connected to the second arc on the right;
- (PS-IV) the third arc on the left is connected to the third arc on the right.

See Figure 3.9.

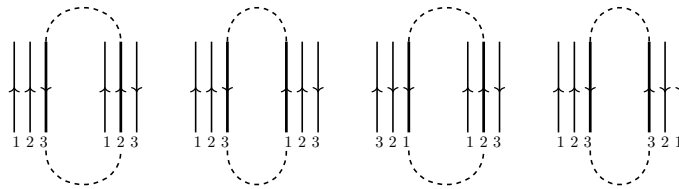


Figure 3.9. Conditions (PS-I)–(PS-IV) for ps-I – ps-IV, respectively.

To perform the bumping pure sliding moves bps-1 and bps-2, we need the following conditions (BPS1) and (BPS2), respectively.

- (BPS1) the second line on the left is connected to the second line on the right,
- (BPS2) the first line on the left is connected to the first line on the right.

Remark 3.1. The pure sliding moves and the bumping pure sliding moves on branched spines are shown in Figure 3.10 and Figure 3.11, respectively.

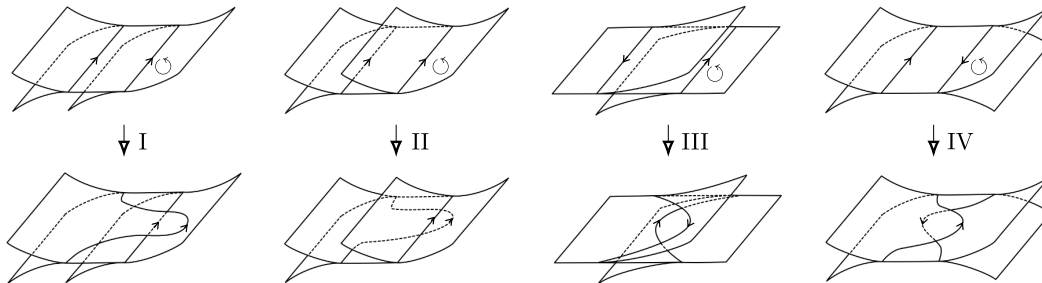


Figure 3.10. Pure sliding moves I–IV on branched spines.

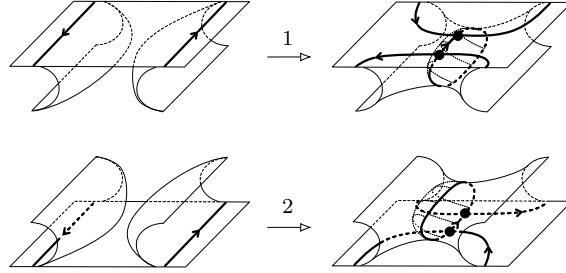


Figure 3.11. Bumping pure sliding moves 1 and 2.

Figure 3.12 shows the correspondence between the three germs of disks at an edge and the three arcs in the circuit diagram. Using this correspondence, we can check that two edges satisfying each of the conditions (PS-I)–(PS-IV) (resp. BPS1, BPS2) correspond to the left-hand sides of the pure sliding moves I–IV (resp. the bumping pure sliding moves 1 and 2) on branched spines.

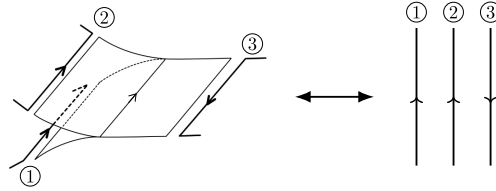


Figure 3.12. Correspondence between the three germs at an edge and the three arcs in the circuit diagram.

Remark 3.2. The four ordered 0–2 moves shown in the top row of Figure 1.7 correspond to pure sliding moves I–IV (Figures 3.6 and 3.10), while the two in the bottom row correspond to bumping pure sliding moves 1 and 2 (Figures 3.7 and 3.11).

3.3. CP move. The *combinatorial Pontryagin move* (in short, *CP move*) is shown in Figure 3.13, which is introduced in [2] to relate different combings of the same 3-manifold.

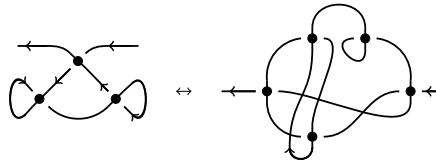


Figure 3.13. CP move.

4. MAIN RESULTS AND PROOFS IN TERMS OF NORMAL O-GRAPHS

4.1. Main results. We denote by \mathcal{M} the set of closed 3-manifolds up to orientation-preserving diffeomorphism. Benedetti and Petronio [2] established a combinatorial description of \mathcal{M} by defining an equivalence relation on closed normal o-graphs.

Theorem 4.1 ([2]). There is a one-to-one correspondence between \mathcal{M} and the set of closed normal o-graphs, up to MP moves, the 0–2 *move* shown in Figure 4.1, and the CP move.

Note that the 0–2 move is a special case of a pure sliding move.

Muramatsu, Taguchi, and the third author [13] proved the following. We choose and fix a preferred MP move among the 16 types of MP moves in Figures 3.1–3.4.

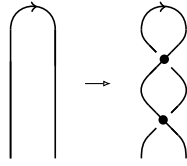


Figure 4.1. 0–2 move.

Theorem 4.2 ([13]). Each MP move can be realized as a sequence consisting of a single preferred MP move (or its inverse), together with pure sliding moves and their inverses.

As a consequence, we obtain the following alternative description of \mathcal{M} .

Corollary 4.3 ([13]). There is a one-to-one correspondence between \mathcal{M} and the set of closed normal o-graphs, up to a preferred MP move, pure sliding moves, and the CP move.

It is natural to ask whether a simpler description of \mathcal{M} exists that does not involve the CP move. Benedetti and Petronio asked [2, Question 9.1.4] whether there is a one-to-one correspondence between \mathcal{M} and the equivalence classes of normal o-graphs with S^2 boundary generated by the 0–2 move, MP moves, and bumping MP moves. Costantino [7, Theorem 3.1] gave an alternative description of \mathcal{M} (in general, for compact oriented 3-manifolds possibly with boundary) by employing *bubble moves* together with bumping MP moves and bumping pure sliding moves.

We fix a preferred move among the 20 types of MP and bumping MP moves in Figures 3.1–3.5. We prove the following proposition in Section 4.3.

Proposition 4.4. The CP move can be realized as a sequence of the preferred move, pure sliding moves, bumping pure sliding moves, and their inverses.

Together with Corollary 4.3, Proposition 4.4 yields the following description of closed 3-manifolds, equivalent to Theorem 2 in the introduction.

Theorem 4.5. There is a one-to-one correspondence between \mathcal{M} and the set of closed normal o-graphs, up to the preferred move, pure sliding moves, and bumping pure sliding moves.

Theorem 4.5 refines Costantino’s result [7, Theorem 3.1] and also gives an affirmative answer to a restricted version of Benedetti and Petronio’s question [2, Question 9.1.3] for closed normal o-graphs. Indeed, each move used in Theorem 4.5 can be obtained as a sequence of the 0–2 move, MP moves, and bumping MP moves, and their inverses (see Remark 4.1).

4.2. Relations among moves. We describe the precise relations among the moves on normal o-graphs. Recall from [13] that the following relations hold among the MP moves and their inverses.

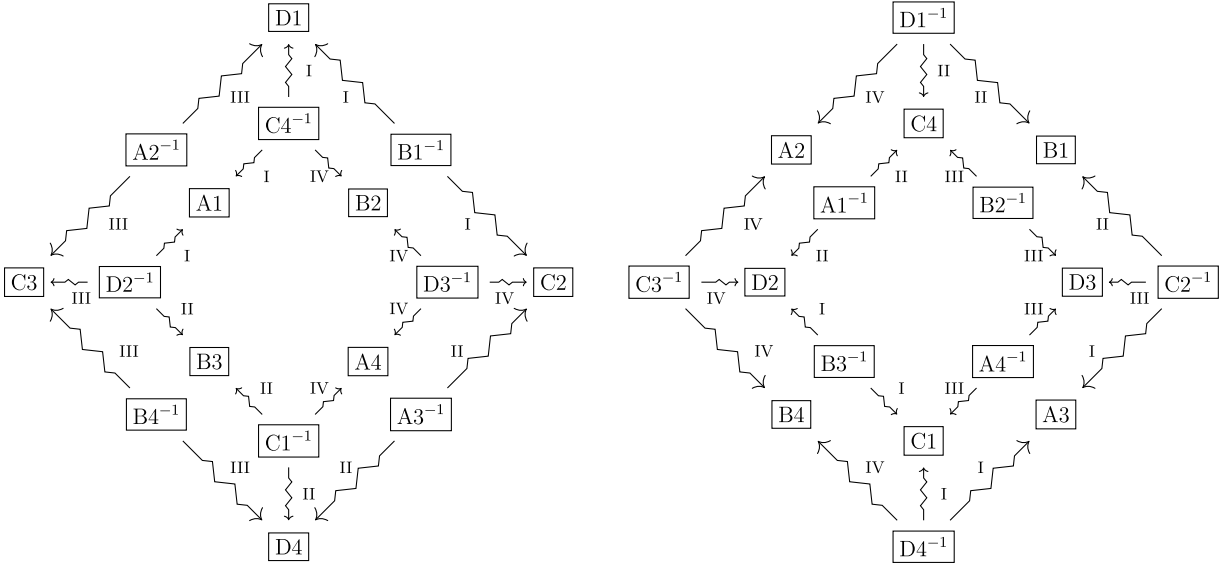


Figure 4.2. Relations among the MP moves. An arrow from a move Y to a move X indicates that X is obtained by composing Y with a pure sliding move. The labels I-IV attached to the arrows indicate the type of pure sliding move. The two MP moves appearing at the same position in the left and right diagrams are inverses of each other, and the arrows at corresponding positions point in opposite directions.

For example, The move $A1$ is sequence of $D2^{-1}$ and ps-I as shown in Figure 4.3.

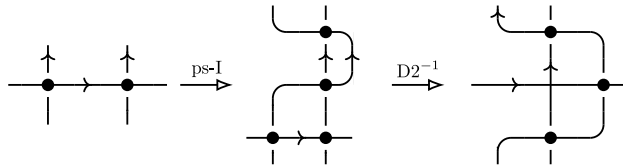


Figure 4.3. Decomposition of $A1$ into ps-I followed by $D2^{-1}$.

Note that, by tracing the decomposition in the opposite direction, from right to left, $A1^{-1}$ decomposes as a sequence of $D2$ followed by the inverse of ps-I. In Figure 4.2, this reverse decomposition allows us to add an arrow in the other diagram at the corresponding position and with the same direction. Similarly, a reverse arrow can be added for each arrow in Figure 4.2. Consequently, each pair of MP moves (and their inverses) in the same diagram is connected by arrows in both directions.

As observed in [13, Remark 2.3], the diagram in Figure 4.2 lacks certain symmetries: in particular, there are no arrows between moves of A-type and B-type. This reflects the asymmetry of branching structures. If we also consider bumping moves, the diagram becomes more symmetric.

Lemma 4.6. Relations involving bumping moves are given in Figure 4.4.

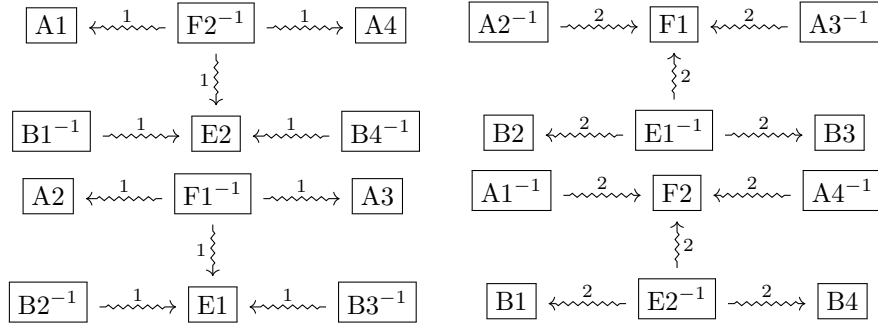


Figure 4.4. Relation involving bumping moves. An arrow from a move Y to a move X indicates that X is decomposed into a bumping pure sliding move followed by Y . The label 1,2 attached to each arrow indicate the type of bumping pure sliding moves.

Proof. The cases of type $B^{-1} \rightsquigarrow E$, $F^{-1} \rightsquigarrow E$, and $F^{-1} \rightsquigarrow A$ are shown in Figures 4.5–4.7, where the orientations of some edges are omitted and are determined by the choice of subtype ($A_1, \dots, A_4, B_1, \dots, B_4, E_1, E_2, F_1, F_2$).

The remaining cases, namely $A^{-1} \rightsquigarrow F$, $E^{-1} \rightsquigarrow F$, and $E^{-1} \rightsquigarrow B$, are obtained similarly by changing the signs of the crossings.

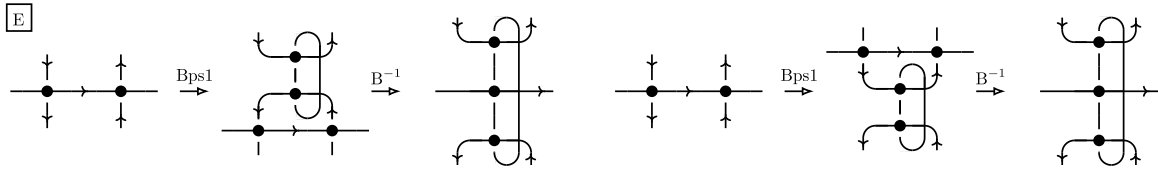


Figure 4.5. Proof of $B_2^{-1} \rightsquigarrow E_1, B_4^{-1} \rightsquigarrow E_2$ (left), $B_3^{-1} \rightsquigarrow E_1, B_1^{-1} \rightsquigarrow E_2$ (right).

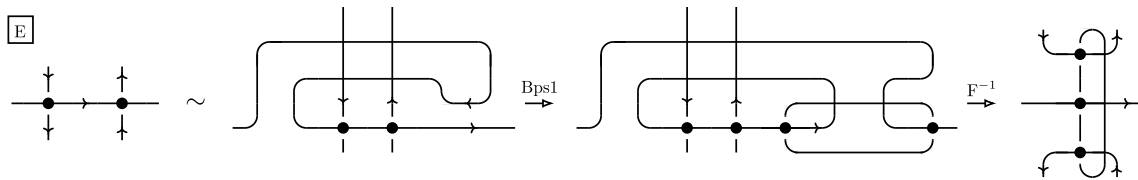


Figure 4.6. Proof of $F_1^{-1} \rightsquigarrow E_1$ and $F_2^{-1} \rightsquigarrow E_2$.

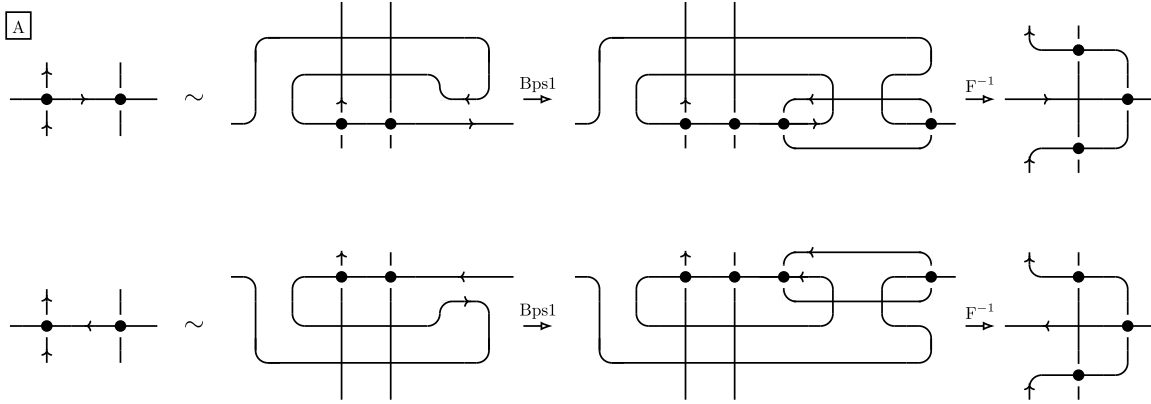


Figure 4.7. Proof of $F_2^{-1} \rightsquigarrow A_1$, $F_1^{-1} \rightsquigarrow A_2$ (top), $F_1^{-1} \rightsquigarrow A_3$, $F_2^{-1} \rightsquigarrow A_4$ (bottom).

□

As in Proposition 4.4, we fix a preferred move among the 20 types of MP and bumping MP moves.

Corollary 4.7. Each bumping MP move can be realized as a sequence consisting of a single preferred move (or its inverse), together with pure sliding moves and bumping pure sliding moves, and their inverses.

Proof. We connect the two diagrams at the top (resp. bottom) in Figure 4.4 to the left (resp. right) diagram in Figure 4.2. By an argument similar to that used above, adding reverse arrows, each pair of boxes in the same diagram is connected by arrows in both directions.

Observe that each type of MP move and bumping MP move appears in either the left or the right diagram, and its inverse appears in the other. Therefore, each bumping MP move can be realized as a sequence consisting of the preferred move or its inverse, together with pure sliding moves, bumping pure sliding moves, and their inverses. □

Remark 4.1. Benedetti and Petronio [2, Lemma 4.5.1] showed that each pure sliding move can be obtained as a sequence of the 0–2 move, MP moves, and their inverses. Similarly, one can prove that each bumping pure sliding move can be obtained as a sequence of the 0–2 move, MP moves, bumping MP moves, and their inverses.

4.3. Proof of Proposition 4.4. By Theorem 4.2 and Corollary 4.7, it suffices to express the CP move as a sequence of MP moves, bumping MP moves, pure sliding moves, and bumping pure sliding moves, together with their inverses.

The sequence realizing the CP move consists of twenty steps. Instead of presenting all intermediate diagrams, we describe it using the Gauss code (E-datum) of normal o-graphs.

Let Γ be a normal o-graph with ordered n vertices. By removing the vertices and joining pairs of opposite edges, one obtains a collection of oriented circuits. We define the number of components of Γ to be the number of such circuits.

Assume first that Γ has one component. The E-datum $\mathcal{E}(\Gamma) = [\mathcal{A}; \gamma]$, where \mathcal{A} is a cyclic permutation of $\{\pm 1, \pm 2, \dots, \pm n\}$ and $\gamma \in \{\pm 1\}^n$ is a sequence of vertex types. The permutation \mathcal{A} records the order in which the vertices are encountered along this circuit, where the sign indicates whether the corresponding branch passes over or under a crossing.

For example, the E-datum $[1, 2, -2, -1; 1, 1]$ corresponds to the normal o-graph shown in Figure 4.8.

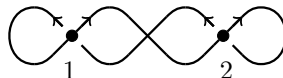


Figure 4.8. Normal o-graph with ordered vertices.

In general, Γ may have several components. In this case, the set $\{\pm 1, \pm 2, \dots, \pm n\}$ is partitioned according to the circuits, and the E-data $\mathcal{E}(\Gamma)$ consists of a cyclic ordering on each part, together with the sequence γ .

To describe local moves, we also use E-data for graphs with open edges, whose endpoints are labeled. For example, the E-data of the left- and right-hand sides of the CP move in Figure 3.13 are given by

$$\text{LHS of the CP move} = [[a, -1, 2, -2, 3, -3, 1, b]; [1, 1, 1]],$$

$$\text{RHS of the CP move} = [[a, -1, -2, 5, -3, 2, 3, 4, -4, 1, -5, b]; [-1, -1, -1, 1, 1]],$$

where, in both sides, the right and left endpoints are labeled by a and b , respectively.

We now describe a sequence of moves connecting these two E-data. Each step is specified by the type of move and the vertices to which it is applied.

Reduction of LHS of the CP move.

$$\begin{aligned} \text{LHS of the CP move} &= [[a, -1, 2, -2, 3, -3, 1, b]; [1, 1, 1]] \\ &\xrightarrow{\text{C3}[2,1]} [[a, 2, -4, -1, -2, 3, -3, 4, 1, b]; [-1, 1, 1, 1]] \\ &\xrightarrow{\text{C3}[2,3]} [[a, 5, 2, -4, -1, 3, -5, -2, -3, 4, 1, b]; [-1, -1, 1, 1, 1]] \\ &\xrightarrow{(\text{ps-I})^{-1}[5,2]} [[a, -3, -1, 2, -2, 3, 1, b]; [-1, 1, 1]] \\ &\xrightarrow{\text{C1}[1,2]} [[a, -3, 2, -4, -1, -2, 3, 1, 4, b]; [1, 1, 1, -1]] \\ &\xrightarrow{(\text{ps-III})^{-1}[1,4]} [[a, -2, 1, -1, 2, b]; [1, 1]] \\ &\xrightarrow{\text{C3}[1,2]} [[a, -1, -2, 3, 1, 2, -3, b]; [-1, 1, 1]] \\ &\xrightarrow{\text{E2}[1,2]} [[-1, -2, -4], [1], [a, 2, 3, 4, -3, b]; [1, -1, 1, -1]] \\ &\xrightarrow{\text{D1}[3,4]} [[-1, -2, -3, -4], [1], [a, 2, 5, 4, -5, 3, b]; [1, -1, -1, -1, 1]] \\ &\xrightarrow{\text{B2}[4,1]} [[-2, -3, -6], [1, 4], [a, 2, 5, -4, 6, -1, -5, 3, b]; [-1, -1, -1, 1, 1, -1]] \\ &\xrightarrow{(\text{bps-2})^{-1}[1,4]} [[-1, -2, -4], [4], [a, 1, 3, -3, 2, b]; [-1, -1, 1, -1]] \\ &\xrightarrow{\text{E1}[1,3]} [[-3, -1, -5], [4], [a, 5, 1, -2, -4, 3, 2, b]; [-1, -1, 1, -1, 1]] \\ &\xrightarrow{(\text{ps-IV})^{-1}[5,1]} [[-2], [3], [a, -1, -3, 2, 1, b]; [-1, 1, -1]] \\ &\xrightarrow{\text{C1}[3,2]} [[-3, -2], [3, 4], [a, -1, 2, -4, 1, b]; [-1, 1, 1, -1]] \\ &\xrightarrow{(\text{bps-2})^{-1}[3,4]} [[a, -1, 2, -2, 1, b]; [-1, 1]]. \end{aligned}$$

Reduction of RHS of the CP move.

$$\begin{aligned} \text{RHS of the CP move} &= [[a, -1, -2, 3, -4, 2, 4, 5, -5, 1, -3, b]; [-1, -1, 1, -1, 1]] \\ &\xrightarrow{\text{F1}[4,5]} [[-5, -4, -6], [4, 2, 6], [a, -1, -2, 3, 5, 1, -3, b]; [-1, -1, 1, -1, 1, 1]] \\ &\xrightarrow{(\text{ps-III})^{-1}[6,4]} [[-4], [2], [a, -1, -2, 3, 4, 1, -3, b]; [-1, -1, 1, 1]] \\ &\xrightarrow{\text{A1}[3,4]} [[-3, -4], [2], [a, -1, -2, 5, 1, 3, -5, 4, b]; [-1, -1, 1, -1, 1]] \\ &\xrightarrow{(\text{bps-1})^{-1}[4,3]} [[-3], [2], [a, -1, -2, 3, 1, b]; [-1, -1, 1]] \\ &\xrightarrow{\text{C1}[2,3]} [[-2, -3], [2, 4], [a, -1, 3, -4, 1, b]; [-1, 1, 1, -1]] \\ &\xrightarrow{(\text{bps-2})^{-1}[2,4]} [[a, -1, 2, -2, 1, b]; [-1, 1]] \end{aligned}$$

Thus we have the assertion.

REFERENCES

- [1] J. E. Andersen and R. Kashaev, *A TQFT from quantum Teichmüller theory*, *Comm. Math. Phys.* **330** (2014), no. 3, 887–934.
- [2] R. Benedetti and C. Petronio, *Branched standard spines of 3-manifolds*, *Lecture Notes in Mathematics*, vol. 1653, Springer-Verlag, Berlin, 1997.
- [3] S. Baseilhac and R. Benedetti, *Quantum hyperbolic invariants of 3-manifolds with $\mathrm{PSL}(2, \mathbb{C})$ -characters*, *Topology* **43** (2004), no. 6, 1373–1423.
- [4] ———, *Classical and quantum dilogarithmic invariants of flat $\mathrm{PSL}(2, \mathbb{C})$ -bundles over 3-manifolds*, *Geom. Topol.* **9** (2005), 493–569.
- [5] ———, *Non ambiguous structures on 3-manifolds and quantum symmetry defects*, *Quantum Topol.* **8** (2017), no. 4, 749–846.
- [6] B. A. Burton, R. Budney, W. Pettersson, and and others, *Regina: Software for low-dimensional topology*, 1999. <http://regina-normal.github.io/>.
- [7] F. Costantino, *A calculus for branched spines of 3-manifolds*, *Math. Z.* **251** (2005), no. 2, 427–442.
- [8] M. Culler, N. Dunfield, M. Goerner, and J. Weeks, *SnapPy, a computer program for studying the geometry and topology of 3-manifolds*. Available at <http://snappy.computop.org>.
- [9] I. Ishii, *Moves for flow-spines and topological invariants of 3-manifolds*, *Tokyo J. Math.* **15** (1992), no. 2, 297–312.
- [10] S. Matveev, *Algorithmic topology and classification of 3-manifolds*, 2nd ed., *Algorithms and Computation in Mathematics*, vol. 9, Springer, Berlin, 2007.
- [11] S. M. Mihalache, S. Suzuki, and Y. Terashima, *The Heisenberg double of involutory Hopf algebras and invariants of closed 3-manifolds*, *Algebr. Geom. Topol.* **24** (2024), no. 7, 3669–3691.
- [12] ———, *Quantum invariants of framed 3-manifolds based on ideal triangulations*. preprint (2022), arXiv:2209.07378.
- [13] K. Muramatsu, S. Suzuki, and K. Taguchi, *On Matveev-Piergallini moves for branched spines*. *arXiv: 2405.18743*. preprint (2021), arXiv:math.GT/2405.18743.
- [14] W. P. Thurston, *The Geometry and Topology of Three-Manifolds*. Princeton University lecture notes, 1978–1981.
- [15] V. G. Turaev and O. Ya. Viro, *State sum invariants of 3-manifolds and quantum 6j-symbols*, *Topology* **31** (1992), no. 4, 865–902.

INTERNATIONAL CENTER FOR MATHEMATICS, DEPARTMENT OF MATHEMATICS, SOUTHERN UNIVERSITY OF SCIENCE AND TECHNOLOGY, SHENZHEN, CHINA

<http://people.mpim-bonn.mpg.de/stavros>

Email address: stavros@mpim-bonn.mpg.de

SECTION DE MATHÉMATIQUES, UNIVERSITÉ DE GENÈVE, 2-4 RUE DU LIÈVRE, CASE POSTALE 64, 1211 GENÈVE 4, SWITZERLAND

<http://www.unige.ch/math/folks/kashaev>

Email address: Rinat.Kashaev@unige.ch

DEPARTMENT OF MATHEMATICAL AND COMPUTING SCIENCE, SCHOOL OF COMPUTING, INSTITUTE OF SCIENCE TOKYO, 2-12-1, OOKAYAMA, MEGURO-KU, TOKYO 152-8552, JAPAN

<https://sakietotera.com>

Email address: sakie@comp.isct.ac.jp